A STUDY OF MOTION EFFECTS AND COMPENSATION TECHNIQUES FOR SYNTHETIC APERTURE RADAR WITH SIMULATION

Cheng-Yen Chiang [*1] and Meng-Che Wu [2]
[1] National Taipei University of Technology
1, Sec. 3, Zhongxiao E. Rd., Taipei 10608 Taiwan
Email: dcychiang@ntut.edu.tw

[2] Taiwan Space Agency
8F, 9 Prosperity 1st Road, Hsinchu Science Park, HsinChu City 300, Taiwan
Email: momo@tasa.org.tw

KEY WORDS: SAR, Motion compensation, Path trajectory simulation, SAR echo simulation

ABSTRACT: The fundamental concept of synthetic aperture radar (SAR) involves combining different instantaneous azimuth positions to simulate a larger antenna, thereby meeting high azimuth resolution requirements. According to SAR processors, the echo signal can be reconstructed to form a focused SAR image. These SAR images need to be calibrated to obtain backscattering coefficients corresponding to the natural land material and structure. As a result, these visually perceivable SAR patterns can be applied to numerous applications.

Due to non-ideal or non-linear platform movements, the accuracy of azimuth position is compromised when utilizing various SAR platforms and data acquisition modes. Without calibration, platform motion can diminish image quality, rendering target identification unreliable. Several motion compensation techniques address this issue, such as "Range tracking" for calibrating slant range movement, the "Phase gradient algorithm" for calibrating azimuth movement using multiple filters, "Entropy minimization" to reduce motion effects through iterations, and intelligent computing algorithms that optimize motion reduction methods.

This study also explores three environments: ground-based, airborne, and spaceborne systems. Due to the challenges associated with collecting real data, echo signal simulations were presented for the three systems. Focusing algorithms specific to each system were also adopted based on the data acquisition types.

In the results, we firstly present simulated SAR echo signals for the three systems, incorporating different motion types, including "ideal trajectory," "measurable motion," and "noisy motion" that cannot be detected by any hardware. Secondly, SAR images with motion compensation are showcased, along with a comparison of different compensation methods. The results indicate that measurable motion is the first stage for compensation. However, in real situations, non-measurable motion is critical in determining image quality, particularly for distributed targets. Thirdly, this study demonstrates the efficacy of intelligent computing algorithms for motion compensation. These intelligent methods effectively address motion issues through intensive computing efforts. Therefore, combining algorithms to address both early and later stages is necessary. Finally, we apply these algorithms to real SAR echo data obtained from ground-based and airborne systems. Motion effects in the spaceborne system are ignored due to the higher platform stability compared to others. In the airborne system, however, motion effects are significant enough to completely compromise the focused SAR image. Depending on the different hardware systems, such as GPS and IMU, suitable methods need to be adopted to restore physical qualities, such as platform altitudes (pitch/roll/yaw angles) and SAR observations (look/squint angles).

Subsequently, a qualitative table is presented to illustrate different environments with motion. Based on this table, the paper concludes by identifying the observation systems and corresponding motion levels that can be ignored.

1. INTRODUCTION

1.1 Motivation

The synthetic aperture radar (SAR) has recently become the most popular tool in the field of remote sensing for Earth's environment. National and commercial SAR systems are operated by various countries for both civil and military purposes. However, one of its major applications is in natural disaster management. In recent years, SAR technology has seen rapid development in terms of spatial and radiometric resolution, observation repeat periods, ground range swath, and other aspects, thanks to high-quality manufacturing. In SAR signal processing, algorithms for new observation modes such as the sliding spotlight and TopoSAR have been developed. Powered by artificial intelligence, deep learning approaches have also been applied to extract information. In this era, we must adapt to new observation types, platforms,

and operational environments. Traditional problems, such as issues related to motion, persist with state-of-the-art equipment.

1.2 Motion issue

In the SAR domain, motion-related issues are consistently the major problem in various types of observation simulations, including those in spaceborne, airborne, or ground environments. These issues can arise from numerous sources in different observation settings. In the spaceborne context, motion is induced by errors in the measurement equipment or inaccuracies in the path trajectory predicted by orbit planning software. In airborne scenarios, motion problems are even more pronounced compared to spaceborne operations. These issues encompass factors such as air drag, engine or motor vibrations due to fuel or battery operation. In fact, the most significant motion problems are encountered in airborne systems, especially those originating from measurement equipment. Depending on the nature of the motion types, whether they are measurable or non-measurable, the associated compensation algorithms need to be adjusted accordingly. In the following sections, we will discuss the sources of motion issues derived from the fundamental coordination transformation process from the platform to the SAR geometry.

2. MOTION COMPENSTATION DEVELOPMENTS

2.1 Motion components

In order to determine the source of motion, it is necessary to perform a coordinate transformation from the local vehicle coordinate system to the SAR geometry. First, we need to define the positional coordinates. The most commonly used coordinate system for representing the vehicle's position is the local Longitude-Latitude-Height (LLH) coordinate system. The relationship between LLH and the East-North-Up (ENU) coordinate system is illustrated in Equation (1):

$$\boldsymbol{P_{enu}} = \begin{bmatrix} x_e \\ y_n \\ z_u \end{bmatrix} = \begin{bmatrix} (\varphi - \varphi_0)(E_b + h)cos\theta \\ (\theta - \theta_0)(E_a + h) \\ h - h_0 \end{bmatrix} \tag{1}$$

The $[x_e, y_n, z_u]^T$ means the XYZ position in ENU coordinate. The E_a and E_b mean the semi-major and semi-minor length of Earth respectively. The φ, θ and h mean the longitude, latitude, and height in LLH coordinate. The zero subscription means the reference position defined by the observation. The transformer of the Euler's rotation angles producing by the pitch, roll, raw angles as in matrix $\boldsymbol{M_1}$ eq(2).

$$\begin{aligned} \boldsymbol{M_1} &= \boldsymbol{R_x}(\gamma)\boldsymbol{R_y}(\alpha)\boldsymbol{R_z}(\beta) \\ &= \begin{bmatrix} cos\alpha\, cos\beta & -cos\alpha\, sin\beta & sin\alpha \\ sin\gamma\, sin\alpha\, cos\beta + cos\gamma\, sin\beta & -sin\gamma\, sin\alpha\, sin\beta + cos\gamma\, cos\beta & -sin\gamma\, cos\alpha \\ -cos\gamma\, sin\alpha\, cos\beta + sin\gamma\, sin\beta & cos\gamma\, sin\alpha\, sin\beta + sin\gamma\, cos\beta & cos\gamma\, cos\alpha \end{bmatrix} \end{aligned} \tag{2}$$

On the other hand, in the SAR geometry, the two important angles defined by the SAR domain are squint and look angle. We also construct those transformer for SAR geometry angles as in $\boldsymbol{M_2}$ eq(3).

$$\boldsymbol{M_2} = \boldsymbol{R_y}(-\theta_\ell)\boldsymbol{R_z}(\theta_{sq}) = \begin{bmatrix} cos\theta_\ell & 0 & -sin\theta_\ell \\ 0 & 1 & 0 \\ sin\theta_\ell & 0 & cos\theta_\ell \end{bmatrix} \begin{bmatrix} cos\theta_{sq} & sin\theta_{Sq} & 0 \\ -sin\theta_{Sq} & cos\theta_{sq} & 0 \\ 0 & 0 & 1 \end{bmatrix} \tag{3}$$

In the eq(3), the θ_ℓ and θ_{Sq} mean the look and squint angle respectively. Base on this transformer, the position of ENU coordinate can be convert into SAR geometry by combination of $\boldsymbol{M_1}$ and $\boldsymbol{M_2}$ as in eq(4).

$$\boldsymbol{P_d} = \begin{bmatrix} d_{LOS} \\ d_{\parallel} \\ d_{\perp} \end{bmatrix} = \boldsymbol{M_2 M_1 P_{enu}} \tag{4}$$

The symbols d_{LOS}, $d_{\parallel}$, and $d_{\perp}$ mean the light-of-sight, parallel, perpendicular components of SAR geometry, we defined it with LPV coordinate[1]. The relationship of $\boldsymbol{P_d}$ and SAR geometry was drawn in the Figure 1 below.

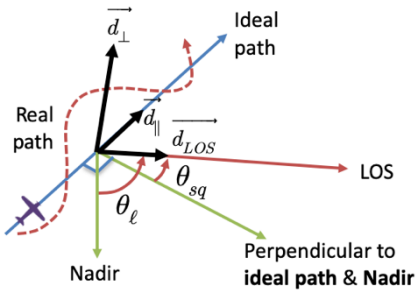

Figure 1. Relationship of LPV coordinate and SAR geometry.

2.2 Motion simulation and analysis

Because the motion is separated into two components, namely the measurable (bias) and non-measurable (noise) components. The non-measurable component is produced due to the mismatch between real motion behavior and measurement data. This mismatch could be induced by equipment errors, such as broken or uncalibrated equipment. Developing a motion compensation algorithm to address these issues is a major concern for data restoration and image quality enhancement. To analyse the compensation issue in more detail, we first need to establish a workflow to generate these motion effects, as shown in Figure 2.

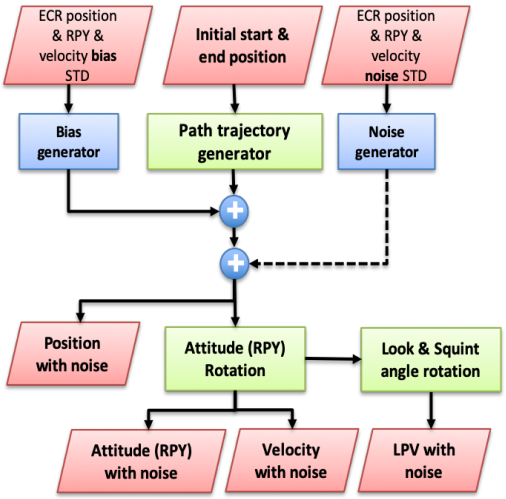

Figure 2. Motion simulation flow-chart.

In Figure 2, before plotting the path trajectory, we only need to initialize the starting and ending positions. Based on the path trajectory prediction method, position points with PRF intervals can be generated. This path trajectory is robust against any noise or bias. Due to the characteristics of SAR geometry, the motion bias can be generated following the LLH in Earth's Fixed Rotation (ECR) coordinates using Euler's angles and velocity. According to the standard deviation assignment, the measured motion is generated. Additionally, we introduce noisy motion data with an assigned standard deviation. By combining both the ideal path trajectory and the noisy motion data, the simulated path trajectory is created. After the simulation, metadata containing all properties of measurable motion is retained, while non-measurable data is discarded.

2.3 Motion compensation approaches

The motion can be addressed using measurable data. However, in real-world scenarios, many motion-related issues can lead to a degradation in image quality. Under special conditions, when non-measurable data dominates, image recognition can become challenging. Therefore, there are several algorithms suitable for addressing these problems, depending on the observation environment and SAR observation modes in use. One of the most popular algorithms is the Range Tracking method[2]. The primary concept behind this method is to maintain coherence among the same targets by tracking prominent point targets at different slant range positions. This helps identify and correct any overall slant range bias, ensuring that the same target stays correctly positioned along the ideal path trajectory. Another method is the Phase Gradient Algorithm (PGA)[3], and the processing flowchart is shown in Figure 3.

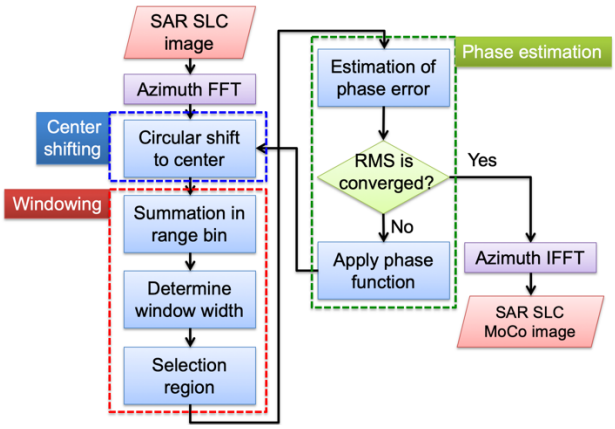

Figure 3. Flow chart of PGA.

In general, the PGA method includes the range tracing method[2] described above for coarse compensation, which is illustrated in the blue dashed rectangular region in Figure 3. Next, windowing processing occurs to reduce the useless region for analysis. After windowing, it is based on the phase error estimation in the slant frequency domain. The phase error is determined through cross-correlation processing. A larger cross-correlation value indicates that there is some error or bias without correction. The compensation equation can be derived from the cross-correlation value. Applying this error to the shifting procedure, the results of the first iteration are represented. This algorithm is applied iteratively. The stopping criterion could be either the minimum phase error or the maximum iteration number. The third compensation method is the minimum entropy method. The main idea of this approach is to find the best image quality index using Shannon's entropy index as shown in eq(5)[4].

$$\tilde{E}(I) = -\sum_{t=1}^{N}\sum_{\eta=1}^{M} I'(t,\eta)\cdot log_{10}[I'(t,\eta)] \quad (5)$$

In the eq(5), the t and η mean the fast and slow time with respective to the slant range and azimuth direction. The $I(t,\eta)$ means the intensity of SAR image after focusing. The $I'(t,\eta)$ is the normalized SAR intensity image. After the definition of image quality index, a lot of artificial intelligence method such as particle swarm optimization algorithm, the simulated annealing, and the ant colony optimization are suitable to solve the motion issue.

2.4 Simulation with point like targets

Based on the motion simulation procedure, we first simulated this motion effect for a point-like target. The purpose of this simulation is to isolate the point target easily for image quality verification. The simulation parameters are shown in Table 1.

Table 1. Point-like target simulation parameters

Item	Value
Carrier freq.	W : 90 [GHz]
TX bandwidth	13 [GHz]
Duration time	0.05 [μsec]
Sampling rate	15 [GHz]
Antenna beamwidth	20 [degrees]
Sensor position interval	0.004 [m]
Sensor height	1.5 [m]
Antenna beamwidth at azimuth	15 [degrees]
Antenna beamwidth at elevation	35 [degrees]
Main beam look angle	50 [degrees]
Motion bias std.	0.05 [m]
Range spacing	0.9993 [cm]
Range resolution	1.1531 [cm]
Azimuth spacing	0.4000 [cm]
Azimuth resolution	0.6326 [cm]

The SAR geometry for those compensation simulation was shown in Figure 4.

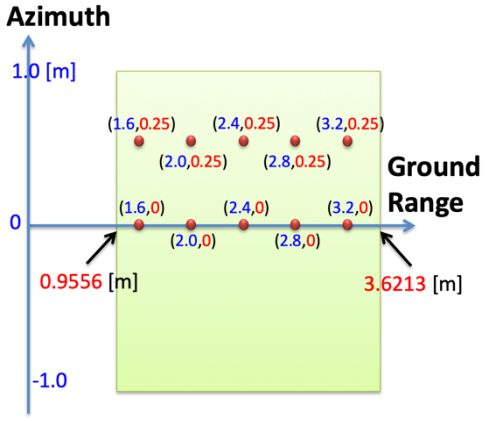

Figure 4. Simulation geometry of 10 point-like targets.

In the indoor chamber environment, we placed 10 point-like targets within a 2-meter azimuthal region, with 4 meters between near and far slant ranges. The positions of the 10 point targets were interleaved at intervals of 0.4 meters. Pairs of targets were located at the same slant range with an azimuthal interval of 0.25 meters. The noise was simulated in LPV coordinates, as shown in Figure 5.

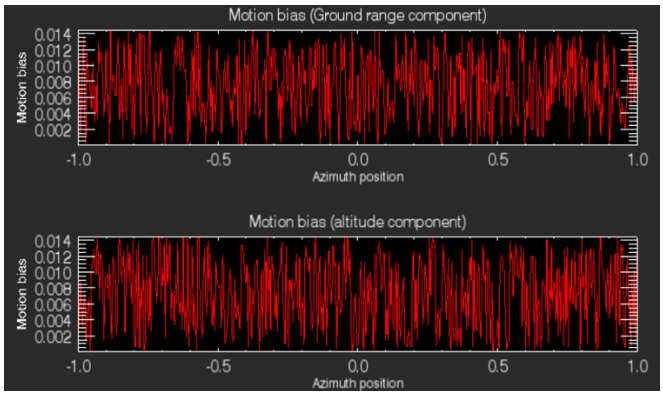

Figure 5. Simulation geometry of 10 point-like targets.

The upper figure in Figure 5 depicts motion with bias and noise along the line of sight, with respect to the azimuthal region from negative one to positive one. The perpendicular component of motion is shown in the bottom of Figure 5. After incorporating the motion effect into the SAR echo signal simulation, the resulting SAR echo signal is displayed in Figure 6.

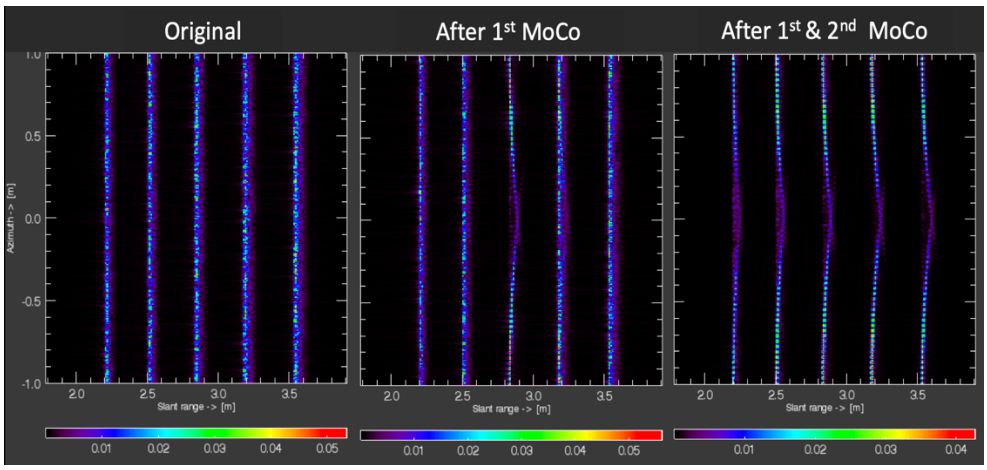

Figure 6. Results of motion compensation.

In Figure 6, the left figure shows the SAR signal in the slant range and azimuth Doppler domain with range compression. As we can see, the range migration effect in the original noisy data is hard to recognize the targets. After the first-order compensation, the global motion problem was solved with corrections made at the reference location, usually placed at the scene's center. The right figure in Figure 6 is the final result, which adds the relative motion components to the central image in Figure 6. After the processing of the first and second compensations, the pattern for different slant ranges can be seen clearly in five lines. In each line, the dash pattern can be figured out as well. This effect is the reason for the double target located at the same slant range distance.

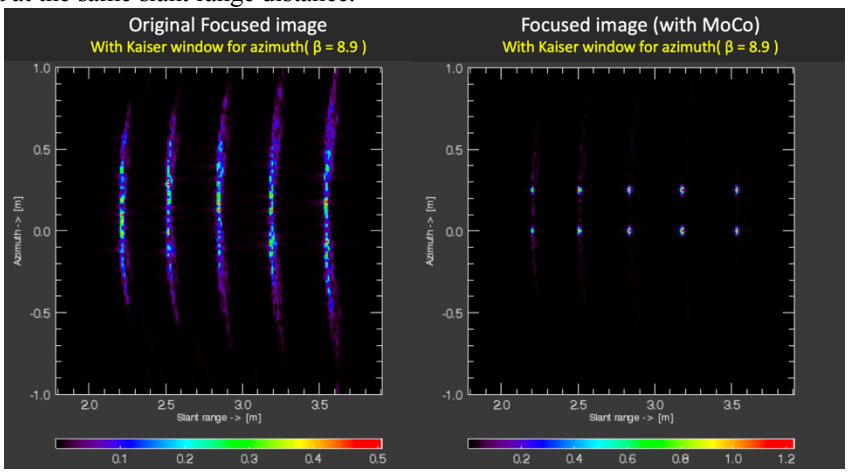

Figure 7. Comparison between original and after motion compensation.

In Figure 7, after displaying the motion-compensated image on the right side of Figure 7, we compare it with the original noisy image. The original image was created using the regular SAR focusing algorithm. However, in this image, apart from azimuth focusing, the range migration effects were not corrected properly.

2.5 Artificial intelligence for motion compensation

For presentation the capability of artificial intelligence for motion compensation, we simulated the distribution target with the ship pattern with those parameters shown in the Table 2[5].

Table 2. Inverse SAR simulation parameters

Item	Value
Carrier freq.	X : 10 [GHz]
TX bandwidth	128 [MHz]
PRF	2 [kHz]
Target rotation velocity	0 [rad/s]
Target moving velocity	15 [m/s^2] = 30 [knot]
Target's moving acceleration	0 [m/s^2]

After SAR echo signal simulation in the inverse SAR geometry environment, conventional focusing procedure also included in this results as shown in the Figure 8.

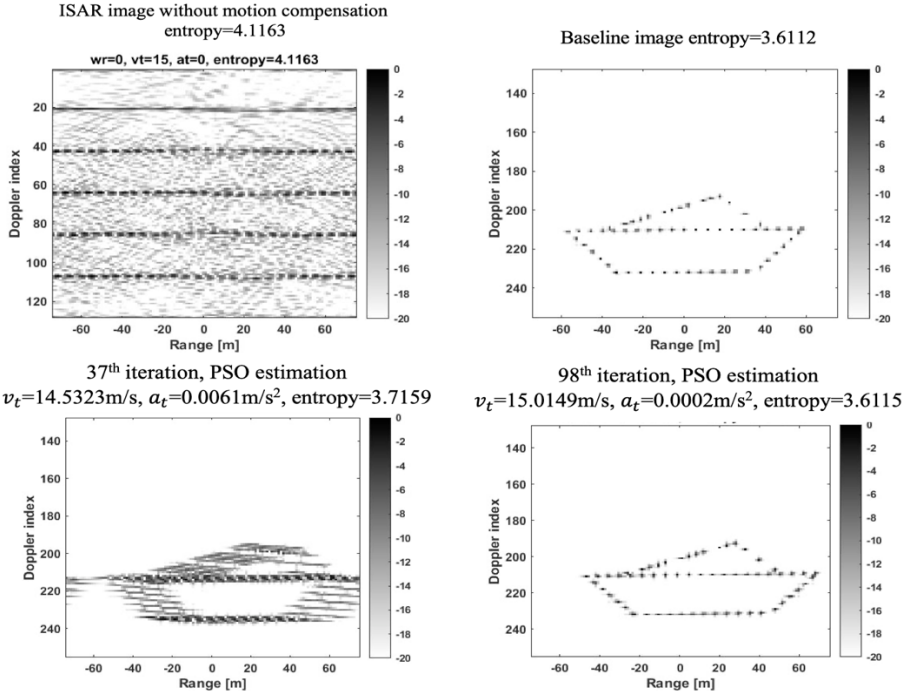

Figure 8. The compensation effect by AI.

In Figure 8, the upper left quadrant displays the noisy image with motion-related issues. The extent of movement is depicted in Table 2, including rotation velocity, linear velocity, and acceleration, among others. The reference image, which exhibits no motion, is presented in the upper right quadrant of Figure 8. Following the application of the particle swarm optimization algorithm, the results of the 37th iteration are displayed in the bottom left quadrant of Figure 8. It is evident that the image quality is subpar due to a lack of coverage. However, by the 98th iteration, the image matches the baseline image, indicating optimal results.

3. CONCLUSION

For this motion compensation study, we have selected robust algorithms for different SAR observation types. Two approaches were adopted for motion compensation in this paper. From a simulation perspective, the results show better effects on image restoration. The noisy image, after conventional stripmap and inverse SAR image processing, exhibited poor quality. By incorporating these algorithms, the image quality can be restored to a useful level. Obtaining real images with known motion problems is very challenging. For future research, more realistic simulated images with scene targets such as urban and natural landscapes will be included in the analysis of this motion compensation process.

4. REFERENCE

[1] K. S. Chen, *Principles of synthetic aperture radar imaging: a system simulation approach*. in Signal and image processing of Earth observations series. Boca Raton London New York: CRC Press, 2016.

[2] John Kirk, “Signal based motion compensation for synthetic aperture radar,” NONE, 764587, Jun. 1999.

[1]

[3] D. E. Wahl, P. H. Eichel, D. C. Ghiglia, and C. V. Jakowatz, “Phase gradient autofocus-a robust tool for high resolution SAR phase correction,” *IEEE Trans. Aerosp. Electron. Syst.*, vol. 30, no. 3, pp. 827–835, Jul. 1994.

[4] Shin, Seung Yong, and Noh Hoon Myung. "The application of motion compensation of ISAR image for a moving target in radar target recognition." *Microwave and Optical Technology Letters*50.6 (2008): 1673-1678.

[5] Chiang, Cheng-Yen, et al. "Simulation of isar motion compensation for moving targets based on particle swarm optimization." *IGARSS 2018-2018 IEEE International Geoscience and Remote Sensing Symposium*. IEEE, 2018.